

## Electronic Supplementary Information

Yoshiaki Miyamoto,<sup>a</sup> Takamichi Matsuno,<sup>a,b,c</sup> and Atsushi Shimojima<sup>\*a,b,c</sup>

*a. Department of Applied Chemistry, Faculty of Science and Engineering, Waseda University, 3-4-1 Okubo, Shinjuku-ku, Tokyo 169-8555, Japan.*

*b. Waseda Research Institute for Science and Engineering, Waseda University, 3-4-1 Okubo, Shinjuku-ku, Tokyo 169-8555, Japan.*

*c. Kagami Memorial Research Institute for Materials Science and Technology, Waseda University, 2-8-26 Nishiwaseda, Shinjuku-ku, Tokyo 169-0051, Japan.*

### **Table of contents**

Fig. S1 Liquid-state <sup>1</sup> H NMR spectrum of the mixture of BTSE, EtOH- <i>d</i> <sub>6</sub> and HCl aq. after stirring at room temperature for 1 h at the molar ratio of BTSE/EtOH- <i>d</i> <sub>6</sub> /H <sub>2</sub> O/HCl = 1:15:20:0.008. ....	3
Fig. S2 (a) GI-SAXS pattern and (b) XRD pattern of the lamellar thin film prepared using TEOS and P123 following ref. 1. ....	3
Fig. S3 SEM images of the lamellar thin film <b>BTSE-P123</b> : (a) cross-section and (b) cross-section and surface of the film. ....	3
Fig. S4 FT-IR spectrum of <b>BTSE-P123</b> . ....	4
Fig. S5 Solid-state <sup>29</sup> Si MAS NMR spectrum of the powder sample of <b>BTSE-DDAB</b> obtained by pulverizing the cast films following ref. 2. ....	4
Fig. S6 TG–DTA curves of (a) powder sample of <b>BTSE-P123</b> obtained by pulverizing the thick films prepared by drop-casting the precursor solution and (b) P123. ....	4
Fig. S7 (a) FT-IR spectra of (black) <b>BTSE-P123</b> and (red) <b>BTSE-P123</b> after removal of P123 by solvent extraction. (b) GI-SAXS pattern and (c) XRD pattern of <b>BTSE-P123</b> after solvent extraction. ....	5
Fig. S8 Nanoindentation load–displacement curves of (green) <b>BTSE-P123</b> , (black) <b>BTSE-DDAB</b> , (red) <b>BTSE-P123</b> after heating at 80 °C for 1 d. ....	6
Fig. S9 AFM surface topographies and elastic modulus maps of the lamellar thin films: (a) <b>BTSE-P123</b> and (b) <b>BTSE-DDAB</b> . ....	7

Fig. S10 (a) Optical microscope images of the crack on <b>BTSE-P123</b> before and after exposure to water vapor (90% RH at room temperature). (b-d) AFM surface topography maps of the healed crack. A narrow, shallow depression (< 1 $\mu\text{m}$ width and $\sim 30$ nm depth) was only observed, which is much smaller than the crack formed by indentation (several micrometers in width and $\sim 800$ nm in depth).....	7
Fig. S11 Schematic image of crack-healing.....	8
Fig. S12 (a) Bending of the film on a PDMS substrate. (b) GI-SAXS pattern of the film ( <b>BTSE-P123</b> ) prepared on a PDMS substrate. (c) Optical microscope images of the film after the first and second crack-healing cycles (90% RH at room temperature). The cracks were formed on the film by bending it with the PDMS substrate.....	8
Fig. S13 (a) XRD patterns of the 2D-hexagonal film prepared using BTSE and P123 (P123/Si= 0.01) measured at different humidities. The inset in panel (a) shows the cross-sectional TEM image of the 2D-hexagonal film. (b) Optical microscope images of the cracks on the 2D-hexagonal film before and after exposure to water vapor (90% RH at room temperature). Cross-sectional TEM images of (c) the cracked area after exposure to water vapor. (d) STEM-EDS mapping of the healed area of the 2D-hexagonal thin film (scale bars: 200 nm). ....	9
Fig. S14 (a) <i>In-situ</i> XRD patterns of the lamellar film prepared using TEOS and P123 measured at different humidities. (b) Optical microscope images of the crack formed on the lamellar film before and after exposure to water vapor (90% RH at room temperature). ....	10
Fig. S15 (a) FT-IR spectra of <b>BTSE-P123</b> before (green) and after (black) heating at 80 $^{\circ}\text{C}$ for 1 d. (b) Optical microscope images of the crack formed on <b>BTSE-P123</b> (heated at 80 $^{\circ}\text{C}$ for 1 d) before and after exposure to water vapor (90% RH at room temperature). ....	10
Fig. S16 (a) XRD pattern of <b>BTSE-P123</b> after immersion in ethanol for 10 min. (b) FT-IR spectra of <b>BTSE-P123</b> before and after immersion in ethanol. ....	11
Fig. S17 TG–DTA curves of the powder samples of (a) <b>BTSE-DDAB</b> and (b) <b>BTSE-P123</b> before and after washing with ethanol. ....	11

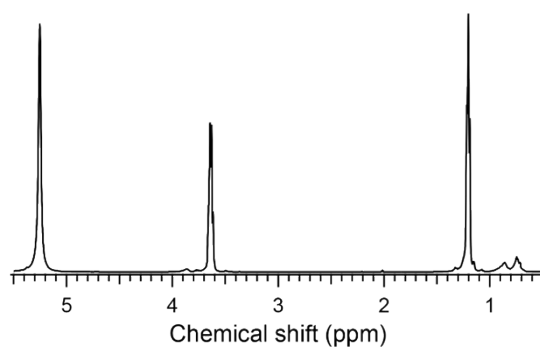


Fig. S1 Liquid-state  $^1\text{H}$  NMR spectrum of the mixture of BTSE,  $\text{EtOH-}d_6$  and  $\text{HCl aq.}$  after stirring at room temperature for 1 h at the molar ratio of  $\text{BTSE/EtOH-}d_6/\text{H}_2\text{O/HCl} = 1:15:20:0.008$ .  $^1\text{H}$  NMR ( $\delta$ , 500 MHz,  $\text{EtOH-}d_6$ ): 0.5–1.0 (4H,  $\text{Si}(\text{CH}_2)_2\text{Si}$ ), 1.20 (18H,  $\text{CH}_3\text{CH}_2\text{O}$ ), 3.64 (12H,  $\text{CH}_3\text{CH}_2\text{OH}$ ), 3.86 (0.21H,  $\text{CH}_3\text{CH}_2\text{OSi}$ ), 5.25 (25H,  $\text{H}_2\text{O}$ ). The relative intensity ratio of  $(\text{CH}_3\text{CH}_2\text{OH})/(\text{CH}_3\text{CH}_2\text{OH} + \text{CH}_3\text{CH}_2\text{OSi})$  confirmed that approximately 98% of the  $\text{SiOEt}$  groups in BTSE were hydrolyzed.

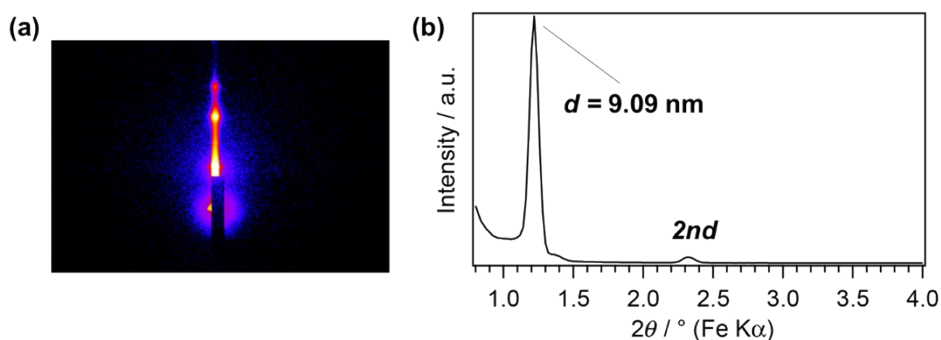


Fig. S2 (a) GI-SAXS pattern and (b) XRD pattern of the lamellar thin film prepared using TEOS and P123 following ref. 1.

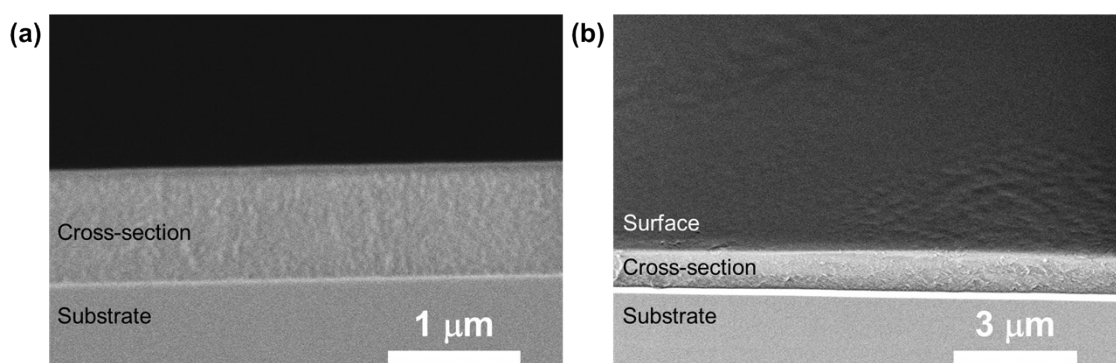


Fig. S3 SEM images of the lamellar thin film **BTSE-P123**: (a) cross-section and (b) cross-section and surface of the film. The film was broken off together with the Si substrate, and the fracture surface was observed without sputter coating.

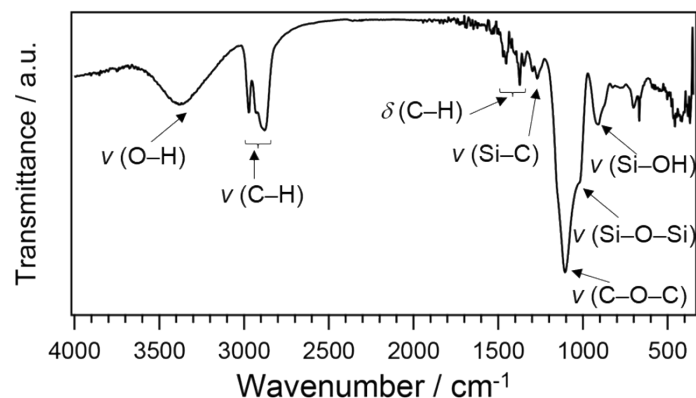
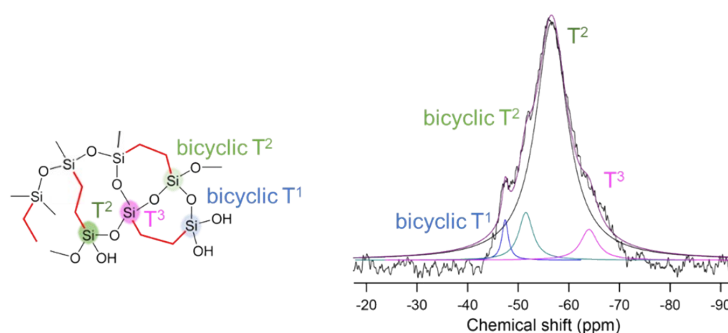


Fig. S4 FT-IR spectrum of **BTSE-P123**.



Assignment	bicyclic T <sup>1</sup>	bicyclic T <sup>2</sup>	T <sup>2</sup>	T <sup>3</sup>
Integral ratio	3	8	84	5

Fig. S5 Solid-state <sup>29</sup>Si MAS NMR spectrum of the powder sample of **BTSE-DDAB** obtained by pulverizing the cast films following ref. 2.

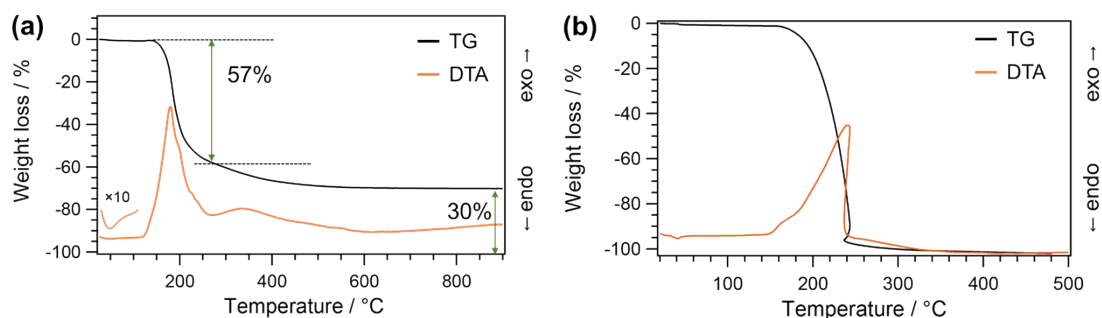


Fig. S6 TG-DTA curves of (a) powder sample of **BTSE-P123** obtained by pulverizing the thick films prepared by drop-casting the precursor solution and (b) P123.

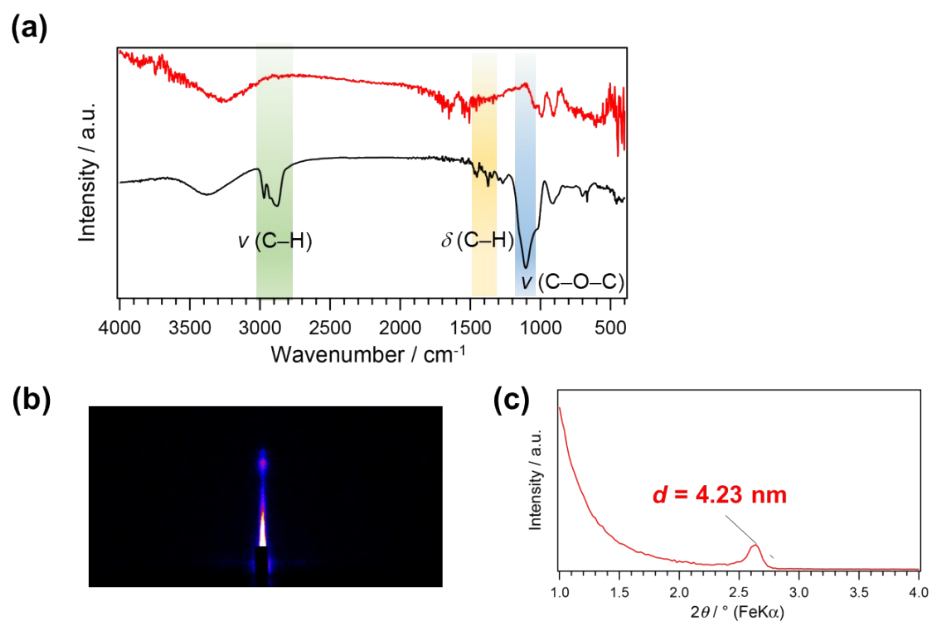


Fig. S7 (a) FT-IR spectra of (black) **BTSE-P123** and (red) **BTSE-P123** after removal of P123 by solvent extraction. (b) GI-SAXS pattern and (c) XRD pattern of **BTSE-P123** after solvent extraction. The solvent extraction was performed by immersing **BTSE-P123** in a mixture of 6N HCl aq. (0.2 mL) and THF (10 mL) at room temperature for 1 d, followed by washing with THF and drying in air.

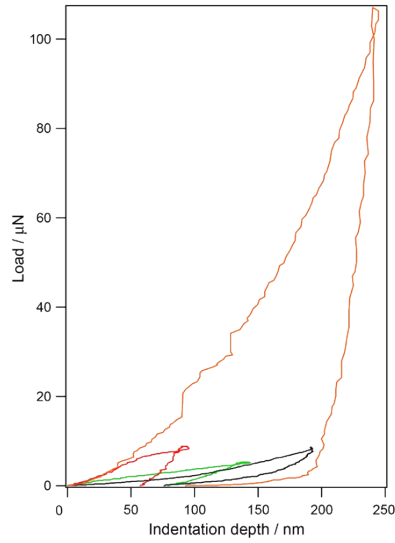


Fig. S8 Nanoindentation load–displacement curves of (green) **BTSE-P123**, (black) **BTSE-DDAB**, (red) **BTSE-P123** after heating at 80 °C for 1 d, and (orange) lamellar thin film prepared using TEOS and P123. Hardness was calculated by the Oliver-Pharr method from the data obtained by continuously measuring the load and displacement during the process of pressing and unloading the triangular pyramidal indenter with an 80° face angle.<sup>3</sup> We used an indenter with a shape factor of  $g = 1.6$  and calculated the projected area of contact at the maximum load  $A_{pml} = gh_c^2$  ( $h_c$ : contact depth). A constant value of  $\varepsilon = 0.75$  was used for the calculation. The hardness of the lamellar film derived from BTSE and DDAB is smaller than the previously reported value. In our previous study,<sup>2</sup> the hardness was calculated to be larger because the shape factor was underestimated.

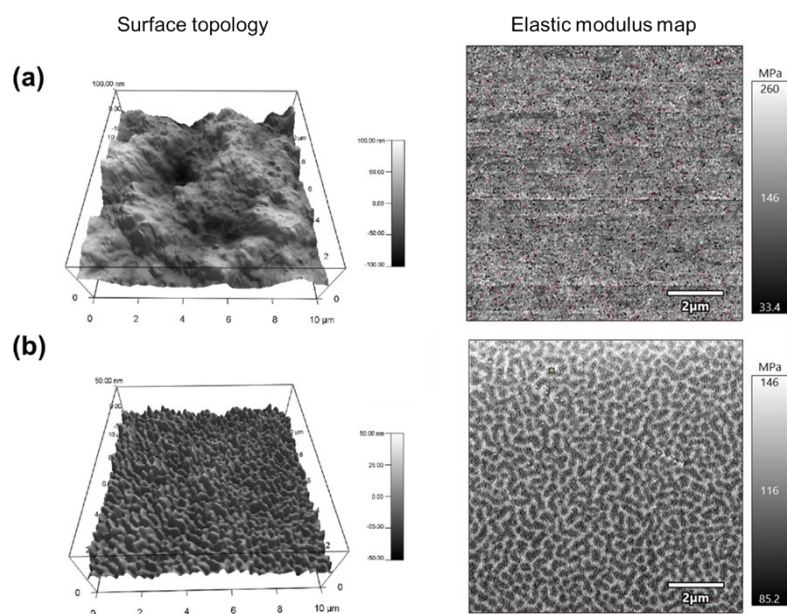


Fig. S9 AFM surface topographies and elastic modulus maps of the lamellar thin films: (a) **BTSE-P123** and (b) **BTSE-DDAB**. Red dots in the elastic modulus map represent non-measurable points.

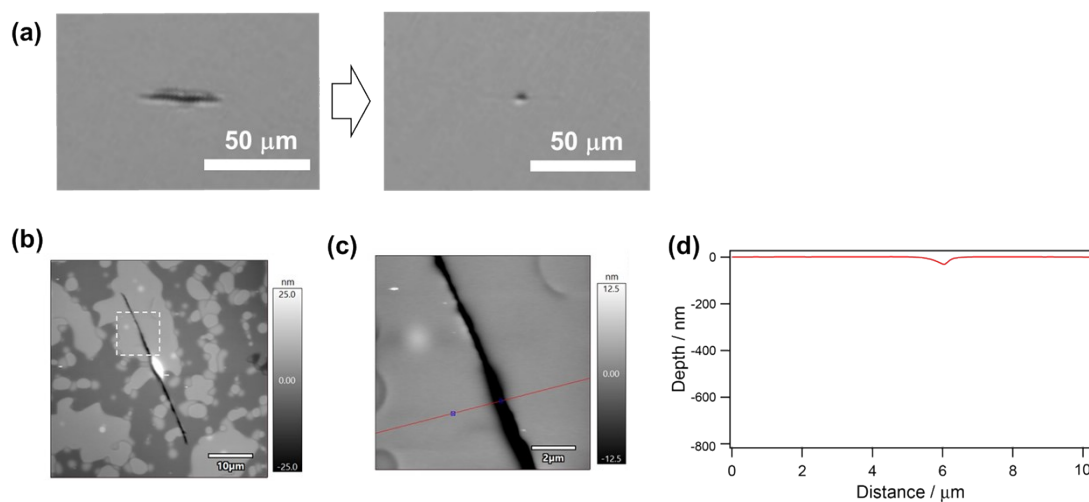


Fig. S10 (a) Optical microscope images of the crack on **BTSE-P123** before and after exposure to water vapor (90% RH at room temperature). (b-d) AFM surface topography maps of the healed crack. A narrow, shallow depression ( $< 1 \mu\text{m}$  width and  $\sim 30 \text{ nm}$  depth) was only observed, which is much smaller than the crack formed by indentation (several micrometers in width and  $\sim 800 \text{ nm}$  in depth).

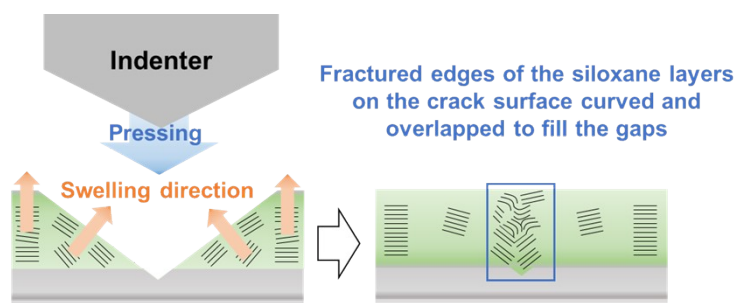


Fig. S11 Schematic image of crack-healing.

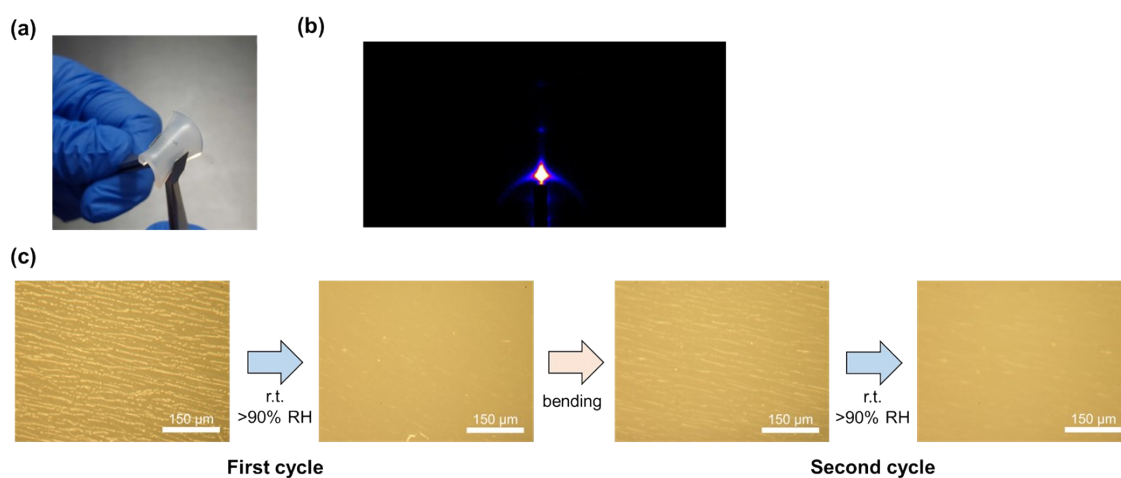


Fig. S12 (a) Bending of the film on a PDMS substrate. (b) GI-SAXS pattern of the film (**BTSE-P123**) prepared on a PDMS substrate. (c) Optical microscope images of the film after the first and second crack-healing cycles (90% RH at room temperature). The cracks were formed on the film by bending it with the PDMS substrate.



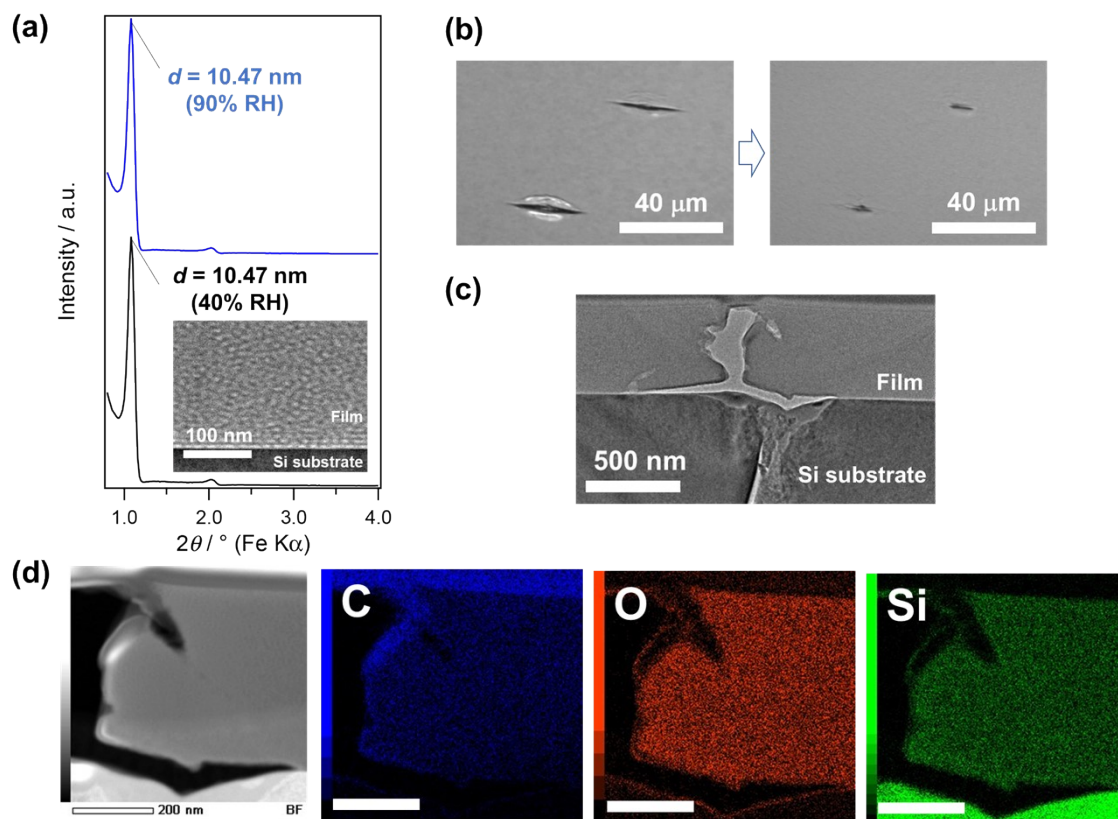


Fig. S13 (a) XRD patterns of the 2D-hexagonal film prepared using BTSE and P123 (P123/Si= 0.01) measured at different humidities. The inset in panel (a) shows the cross-sectional TEM image of the 2D-hexagonal film. (b) Optical microscope images of the cracks on the 2D-hexagonal film before and after exposure to water vapor (90% RH at room temperature). (c) Cross-sectional TEM image of the cracked area after exposure to water vapor. (d) STEM-EDS mapping of the healed area of the 2D-hexagonal thin film (scale bars: 200 nm).

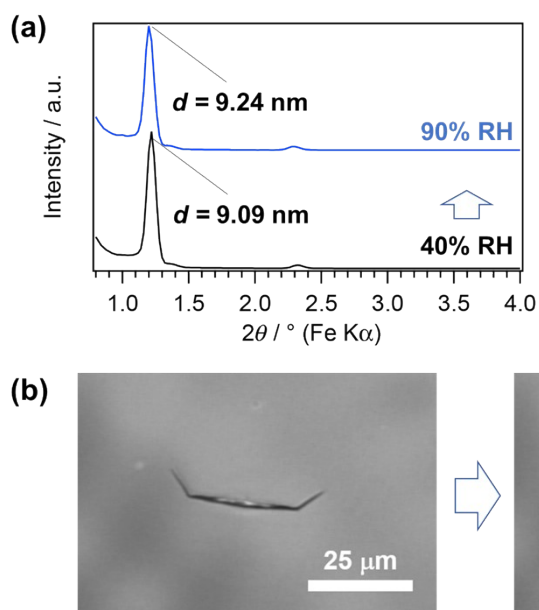


Fig. S14 (a) *In-situ* XRD patterns of the lamellar film prepared using TEOS and P123 measured at different humidities. (b) Optical microscope images of the crack formed on the lamellar film before and after exposure to water vapor (90% RH at room temperature).

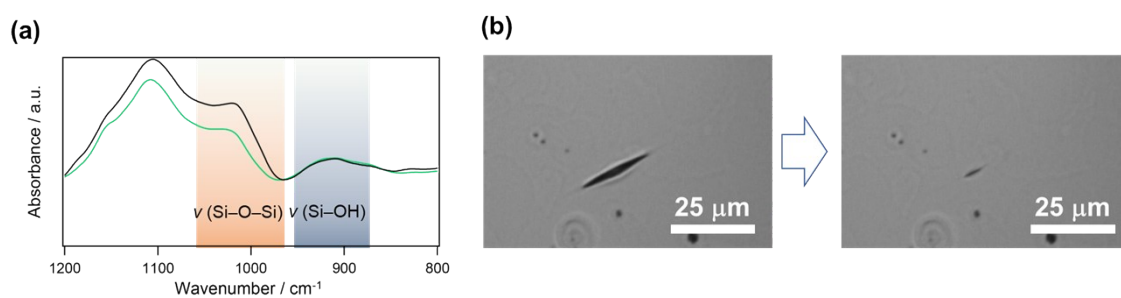


Fig. S15 (a) FT-IR spectra of **BTSE-P123** before (green) and after (black) heating at 80 °C for 1 d. (b) Optical microscope images of the crack formed on **BTSE-P123** (heated at 80 °C for 1 d) before and after exposure to water vapor (90% RH at room temperature).

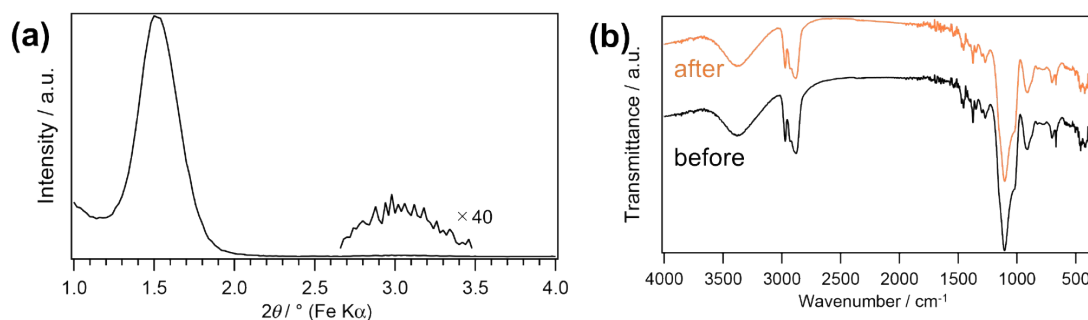


Fig. S16 (a) XRD pattern of **BTSE-P123** after immersion in ethanol for 10 min. (b) FT-IR spectra of **BTSE-P123** before and after immersion in ethanol.

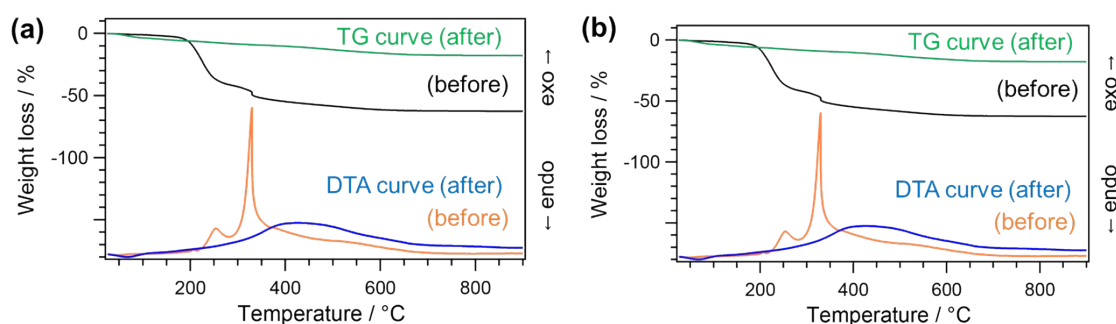


Fig. S17 TG-DTA curves of the powder samples of (a) **BTSE-DDAB** and (b) **BTSE-P123** before and after washing with ethanol. The samples were washed twice with ethanol, collected by centrifugation, and dried overnight under reduced pressure.

Movie S1 Healing of the crack formed on the lamellar film prepared using BTSE and P123 (**BTSE-P123**). The crack was formed by pressing a Knoop indenter on the film with a load of 147 mN at 25 °C and 55% RH. The cracked film was exposed to water vapor (at 25 °C and 90% RH) after removal of the indenter and observed by an optical microscope.

Movie S2 Healing of the crack formed on the lamellar film prepared using BTSE and P123 (**BTSE-P123**) after immersion in ethanol for 10 min. The crack was formed by pressing a Knoop indenter on the film with a load of 147 mN at 25 °C and 48% RH. The cracked film was exposed to water vapor (at 25 °C and 90% RH) after removal of the indenter and observed by an optical microscope.

## References

1. C.-W. Wu, J.-B. Pang and M. Kuwabara, *Chem. Lett.*, 2002, **31**, 974.
2. S. Kodama, Y. Miyamoto, S. Itoh, T. Miyata, H. Wada, K. Kuroda and A. Shimojima, *ACS Appl. Polym. Mater.*, 2021, **3**, 4118.
3. E. Broitman, *Tribol. Lett.*, 2017, **65**, 23.